UV Absorption Spectrum and Photodissociation Channels of the Simplest Criegee Intermediate (CH$_2$OO)

Richard Dawes,*,[†] Bin Jiang,[‡] and Hua Guo*,[‡]

[†]Department of Chemistry, Missouri University of Science and Technology, Rolla, Missouri 65409, United States
[‡]Department of Chemistry and Chemical Biology, University of New Mexico, Albuquerque, New Mexico 87131, United States

S *Supporting Information*

ABSTRACT: The lowest-lying singlet states of the simplest Criegee intermediate (CH$_2$OO) have been characterized along the O–O dissociation coordinate using explicitly correlated MRCI-F12 electronic structure theory and large active spaces. It is found that a high-level treatment of dynamic electron-correlation is essential to accurately describe these states. A significant well on the *B*-state is identified at the MRCI-F12 level with an equilibrium structure that differs substantially from that of the ground *X*-state. This well is presumably responsible for the apparent vibrational structure in some experimental UV absorption spectra, analogous to the structured Huggins band of the iso-electronic ozone. The *B*-state potential in the Franck–Condon region is sufficiently accurate that an absorption spectrum calculated with a one-dimensional model agrees remarkably well with experiment.

Criegee intermediates[1] (R$_1$R$_2$COO or CIs) arise from ozonolysis of biogenic and anthropogenic alkenes, which is an important process in the atmosphere.[2] The nascent CIs are internally hot and decay quickly. As a result, their direct detection and characterization have been frustrated until very recently. Thanks to breakthroughs in generating these elusive species in the gas phase,[3,4] the last two years have witnessed an explosion in activity on their structures, spectroscopy, and reactivity.[5] For example, the structure of the simplest CI (CH$_2$OO) in its ground electronic state has been measured by microwave spectroscopy and closely matched by theoretical calculations.[6,7] Infrared spectroscopy[8] and calculations[9] of the vibrational spectrum are also in close accord. Very recently, the unimolecular decay of CH$_3$CHOO to the OH radical has been investigated by overtone excitations.[10] Perhaps most importantly, kinetic measurements have revealed that collision stabilized CIs can react rapidly with itself[11] as well as key atmospheric species such as H$_2$O, NO$_2$, and SO$_2$, thus dramatically impacting our current understanding of atmospheric chemistry.[12]

In addition to the uni- and bimolecular reactions mentioned above, CIs can be efficiently removed from the atmosphere by absorbing a solar UV photon near 340 nm.[13−18] As a result, the rate of CI photodissociation influences the kinetics of its reactions. The electronic transition associated with the UV absorption and the subsequent dissociation are currently not well understood and thus the subject of vigorous investigations.

Taking CH$_2$OO as an example, the strong UV absorption is attributed to the B ^{1}A′ ← X ^{1}A′ transition, leading to photofragments in two spin-allowed channels. The lower energy channel forms singlet fragments: H$_2$CO(X ^{1}A$_1$) + O(^{1}D), while a higher energy channel leads to triplet fragments: H$_2$CO(a ^{3}A″) + O(^{3}P). Due to the transient nature of the CI, the UV absorption spectrum is challenging to measure experimentally and significantly different results have been obtained by three groups. In 2012, Beames et al. reported a strong UV absorption band in the 300−370 nm range.[13] No vibrational structure was resolved, and a fit to a simple Gaussian form was interpreted as evidence for a purely repulsive B-state. However, the 2013 measurements by Sheps yielded a spectrum with the band maximum shifted to a slightly lower energy (longer wavelength) and, provocatively, extending much further on the low-energy wing with a series of oscillations that appear to be vibrational structure (possibly suggestive of bound levels on the B-state).[16] These would be analogous to the structured Huggins band assigned to the B-state in the iso-electronic ozone system.[19] In 2014, Ting et al. reported another measurement of the UV spectrum.[17] There, the band maximum lies closer to that obtained by Beames et al.,[13] but on the low-energy side the spectrum extends to longer wavelengths and exhibits similar apparent vibrational structure to that reported by Sheps.[16] Interpretation of the various measurements has been the source of considerable speculation regarding fundamental aspects of the states and dynamics of the system as well as the different types of experimental measurements and conditions (the jet-cooled conditions of Beames et al. ($T \sim 10$ K) were different from the thermal conditions ($T \sim 300$ K) of the other two experiments).

While the photochemistry of CIs has been studied from first-principles,[13,14,20,21] only two quantum dynamics studies appearing in the literature recently presented calculations of the UV spectrum[22,23] and photodissociation channels.[23] The study by Samanta et al. involved two-dimensional (2D) wave packets in the (r_{OO}, r_{CO}) coordinates using quasi-diabatic states based on cuts through the nine-dimensional (9D) potential energy surfaces (PESs) of the excited states at the dynamically weighted complete active space self-consistent field (DW-CASSCF) level.[24] Their predicted UV absorption spectrum is broad, featureless, and centered at a much higher energy than any of the experimental spectra. The predictions for their 2D and a further reduced 1D model were very similar. On the

other hand, the study by Meng and Meyer was 9D using the multilayer multiconfigurational time-dependent Hartree approach, but with a quadratic vibronic Hamiltonian.[22] Their predicted UV spectrum has a maximum much closer to the experiments, thanks to the multireference configuration interaction (MRCI) treatment of electronic structure. However, the calculated absorption spectrum is much narrower than experiments and its strong oscillations do not match any of the experiments, especially on the low-energy wing where the possible vibrational structure was found. As discussed below, neither of these theoretical models is adequate to accurately describe the electronic structure and/or dynamics of the CI.

Combining the three lowest states of formaldehyde: $H_2CO(X\ {}^1A_1,\ a\ {}^3A'',\ A^1A'')$, with the three lowest states of atomic oxygen: $O({}^3P,\ {}^1D,\ {}^1S)$, yields a total of 15 singlet molecular states for CH_2OO. A complete determination of the relevant excited state PESs and their couplings in full-dimensionality is beyond the scope of this Communication, and we will instead provide key characteristics of the excited-state PESs along the r_{OO} dissociation coordinate. Most of the calculations discussed here maintained planar geometries (C_S symmetry, $8\ {}^1A' + 7\ {}^1A''$ electronic states).

To provide a well-converged description of the excited-state electronic structure, it is imperative to include the dynamical correlation with a large active space. To this end, our DW-CASSCF models employed a full-valence (18e, 14o) active space, and they provide a reference for explicitly correlated (F12) MRCI calculations.[25,26] The F12 methods include explicit functions of the interparticle distances in the wave function, which greatly improves the convergence of dynamic electron-correlation with basis set, yielding near complete basis set quality results with relatively small bases.[27] Additional calculations are presented in Supporting Information (SI). To test the accuracy of the DW-CASSCF/MRCI-F12 strategy, a few MRCI-F12 points were obtained along the r_{OO} dissociation coordinate in the ground electronic state, relaxing all other coordinates. These calculations used a dynamic weighting procedure[28] with weight $W(E_i) = \mathrm{sech}^2(|E_{ref} - E_i|/\beta)$ focused on the ground X-state with a weight parameter (β = 3.0 eV). At the equilibrium geometry the relative weights of the X-, A-, and B-states are 1.00, 0.43, 0.15. The MRCI geometries are very similar to those obtained at the CCSD(T*)-F12b/VTZ-F12 level, as shown in SI, validating the MRCI approach.

We first computed the excited-state energies along the series of relaxed geometries on the X-state so obtained. For the excited states, however, the maximum weight in the generalized DW scheme[28] was placed on the B-state diabat, while states both above and below received lesser weights according to β = 3.0 eV. Thus, at the Franck−Condon (FC) point for the B-state-focused calculation the relative weights of the X-, A-, and B-states are 0.25, 0.81, 1.00, helping to achieve better convergence of the B-state. This is in contrast to the weights of 1.000, 0.092, 0.014 obtained with β = 2.0 eV focused on the X-state as reported by Samanta et al.[23] Thus, the X- and B-states were each individually optimized with maximal weight on the state of interest for each calculation. The MRCI-F12 results are not sensitive to the choice of weight parameter β used in the preceding CASSCF calculation.

Figure 1 shows the behavior of the $^1A'$ states along the relaxed dissociation coordinate to the lower product channel. The vertical excitation energy (3.751 eV) is very close to that reported by Beames et al.[13] (3.70 eV) and slightly lower than the values calculated by Meng and Meyer[22] using standard
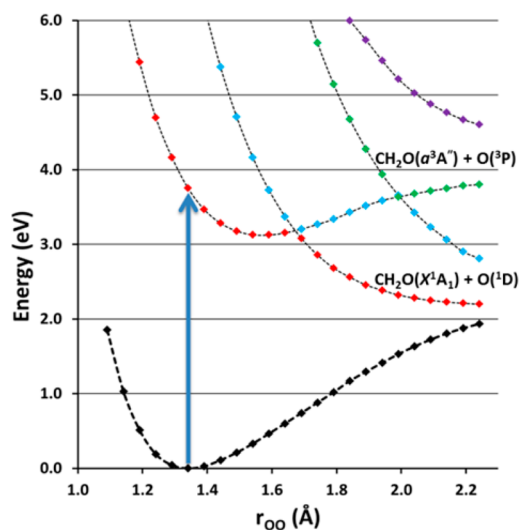

Figure 1. Scan along r_{OO} showing energies at the MRCI-F12 level for the lowest five $^1A'$ states for geometries relaxed along the ground state (see text). Transition to B-state is indicated by blue arrow, with an excitation energy of 3.751 eV.

MRCI/AVTZ (presumably due to the improved convergence *wrt* basis set of MRCI-F12 and the use of a larger active space). The MRCI-F12 values are very well-converged at the VTZ-F12 basis set level (negligible differences were seen in tests using the larger VQZ-F12 basis). Core-correlation effects were also found to be negligible. In terms of the excitation energy, the full-valence active space used in parts of this study was likely unnecessary as very similar results are obtained if the active space is restricted by closing the 2s orbitals on C and O atoms (12e, 11o).

Figure 2 displays the calculated absorption spectrum using a 1D model and the B-state adiabat shown in Figure 1. The
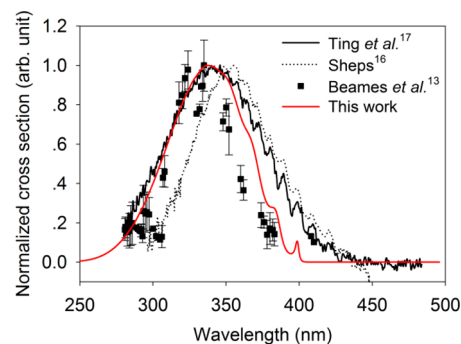

Figure 2. Calculated UV absorption spectrum using a 1D model and PESs shown in Figure 1 are compared to the three experimental spectra. Only the ground vibrational state of $CH_2OO(X)$ was used in the calculation.

spectrum was obtained using the Chebyshev real wave packet method,[29] and more details of the calculations can be found in SI. The calculated spectrum is remarkably close to the experimental measurements in terms of the excitation energy and shape. Furthermore, it possesses a weak oscillatory structure in the long wavelength wing of the absorption spectrum, as observed by Sheps[16] and Ting et al.[17]

The remarkable theoretical result in Figure 2 suggests that deficiencies in the level of electronic theory are the main reasons for the discrepancies with the model of Samanta et al.[23]

Specifically, the chosen CASSCF method does not capture enough dynamic electron-correlation to be accurate. This is confirmed by our own calculations, which show that at the CASSCF level, the B-state PES in the FC region is much too high, too repulsive, and lacks a pronounced well at larger r_{OO} observed in a high-level electron-correlation treatment such as MRCI-F12. Samanta et al. also reported disruptions in the electronic structure calculations near each of two locations where the B-state diabat is crossed by repulsive states (both correlating to the lower exit channel). Their use of DW-CASSCF focused maximum weight on the ground state, which results in a less well-converged B-state and an even larger excitation energy. We prefer an extension of the DW procedure in which maximum weight is assigned to the state of interest (in this case the B-state).[28] This results in better and more robust convergence (no disruptions) and permitted a fine-grained scan of the crossing regions and analysis of the nonadiabatic coupling matrix elements, as discussed below.

The Meng−Meyer model[22] is also deficient. First, their (8e, 8o) active space may be too restrictive. Analysis of the B-state electronic structure at the FC point indicates that the (8e, 8o) active space does include the dominant configurations, but unphysical behavior emerges at larger r_{OO} as the two crossings of the B-state diabat are frustrated and the exit channel degeneracies are not correctly captured. The first crossing is fairly far away at $r_{OO} > 1.6$ Å and so it is not clear whether the small active space is significantly impacting the topography of the B-state in the FC region. In addition, the harmonic expansion of the PES only gives an approximation of the PES in the FC region, which likely results in the narrow spectral width and the strong oscillatory structure.

It is clear from Figure 1 that a significant well exists in the B-state when dynamic electron-correlation is treated with MRCI-F12. (This well is not significant at the CASSCF level,[23] but found in some DFT calculations.[21]) However, following the B-state diabat by eye through the two crossing points toward the asymptote is somewhat deceptive. Along the cut shown in Figure 1, the B-state appears entirely bound relative to the vertical excitation energy (except by nonadiabatic paths to the lower channel). In fact triplet formaldehyde has such a significantly different equilibrium geometry from the singlet form (e.g., r_{CO} is elongated by >0.1 Å), that a relaxed scan of the B-state is necessary in order to appreciate the energetics of the upper channel asymptote more clearly.

Figure 3 shows a relaxed (but planar) cut along r_{OO} of the B-state at the MRCI-F12/VTZ-F12 level with DW-CASSCF (12e, 11o) reference wave function. The equilibrium geometry on the B-state differs significantly from its ground-state counterpart (given in parentheses below) mainly in three coordinates. The r_{OO} and r_{CO} bond distances are both significantly longer [$r_{OO} = 1.564$ (1.341) Å, $r_{CO} = 1.340$ (1.269) Å], and the ∠COO angle is much smaller 99.4 (117.9)°. Lee et al. also reported large differences in these three coordinates in their DFT calculations. Their calculated FC band envelop for UV absorption is however centered at significantly shorter wavelength than the experiments. The optimized geometry at the B-state minimum is planar, but asymptotically, the equilibrium structure of the triplet formaldehyde wags the methylene H atoms ∼35° out-of-plane. This additional relaxation was computed to be 0.080 eV at the UCCSD(T*)-F12b/VTZ-F12 level. Thus, a fully relaxed asymptote in Figure 3 would be slightly lower still. Nevertheless, the calculated well on the B-state is substantial with D_e
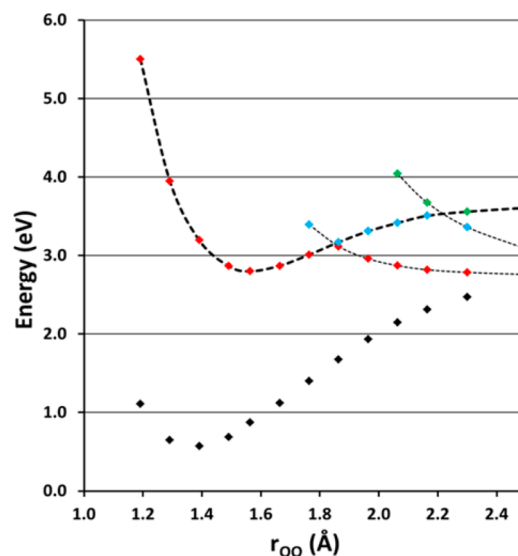

Figure 3. Scan along r_{OO} showing energies at the MRCI-F12 level for the lowest four $^1A'$ states at planar geometries relaxed along the B-state. Minimum is at 2.80 eV relative to ground-state minimum. Asymptotically, the out-of-plane wag of triplet H_2CO lowers the energy by another ∼0.080 eV (see text).

∼ 0.741 eV (5980 cm^{-1}), so the existence of bound states is anticipated. The calculated values and experimental measurements are all consistent with each other and with the known energy gaps between fragment states. The estimated dissociation energy of CH_2OO in the ground electronic state is $D_0 \leq 2.04$ eV,[15] which, combined with the well-known singlet−triplet gaps in formaldehyde ($T_0(H_2CO) = 3.12$ eV) and O atom ($O(^1D) - O(^3P) = 1.97$ eV), makes $O(^3P)$ potentially observable at 3.19 eV (389 nm), or even lower. See SI for additional discussion of D_0.

The existence of a B-state well apparently impacts the absorption spectrum, as some recurrence of the wave packet leads to the weak oscillations at long wavelengths. A quantitatively accurate absorption spectrum would have to move beyond the 1D model by performing quantum dynamics on multidimensional nonadiabatically coupled PESs.

Experimentally, upon photodissociation, product fragments corresponding to both channels have been observed, e.g., $O(^1D)$ and $O(^3P)$ (M. I. Lester, personal comm.). A detailed characterization of the products and their branching ratios is not yet available but is expected to be a sensitive probe of the character of the states and the nature of the nonadiabatic couplings. As shown in Figure 3, two crossings of the B-state diabat lead to the lower-energy product channel.

In SI, a fine-grained scan of the crossing regions is presented including the nonadiabatic coupling. There it is shown that the coupling at the second (longer r_{OO}) crossing point is much broader and causes a significant deflection of the adiabats (minimum gap is 234 cm^{-1}). These nonadiabatic crossings are vital for a first-principles description of the dissociation dynamics which will be the subject of a follow-up study.

To summarize, we have performed a high-level study of the singlet states of the simplest CI CH_2OO relevant to recent experimental studies of the UV absorption spectrum and photodissociation dynamics. We find that a high-level treatment of dynamic electron-correlation such as MRCI-F12 is essential to understand the nature and topography of these states. The vertical excitation energy to the B-state is predicted at 3.751 eV,

which is very close to experiment. A calculated UV absorption spectrum using a 1D model matches the experiments remarkably well given the limitations of the model. We have characterized the two crossing regions and found much more significant nonadiabatic coupling at the second (longer r_{OO}) crossing point. A significant well ($D_e = 5980$ cm^{-1}) was located on the B-state with an equilibrium geometry differing significantly in three coordinates from that of the ground state, and it is responsible for the weak oscillations in the absorption spectrum at long wavelengths. We expect that a theoretical study capable of fully reproducing the apparent vibrational structure found in some of the spectra and making accurate predictions of product branching ratios will require three excited-state quasi-diabatic PESs with at least three active coordinates.

■ ASSOCIATED CONTENT

ⓢ Supporting Information

Additional details and comparisons of the electronic structure methods and the 1D quantum dynamics model. This material is available free of charge via the Internet at http://pubs.acs.org.

■ AUTHOR INFORMATION

Corresponding Authors
dawesr@mst.edu
hguo@unm.edu

Notes
The authors declare no competing financial interest.

■ ACKNOWLEDGMENTS

■ REFERENCES

(1) Criegee, R. *Angew. Chem., Int. Ed.* **1975**, *14*, 745.
(2) Johnson, D.; Marston, G. *Chem. Soc. Rev.* **2008**, *37*, 699.
(3) Welz, O.; Savee, J. D.; Osborn, D. L.; Vasu, S. S.; Percival, C. J.; Shallcross, D. E.; Taatjes, C. A. *Science* **2012**, *335*, 204.
(4) Taatjes, C. A.; Welz, O.; Eskola, A. J.; Savee, J. D.; Scheer, A. M.; Shallcross, D. E.; Rotavera, B.; Lee, E. P. F.; Dyke, J. M.; Mok, D. K. W.; Osborn, D. L.; Percival, C. J. *Science* **2013**, *340*, 177.
(5) Taatjes, C. A.; Shallcross, D. E.; Percival, C. J. *Phys. Chem. Chem. Phys.* **2014**, *16*, 1704.
(6) Nakajima, M.; Endo, Y. *J. Chem. Phys.* **2013**, *139*, 101103.
(7) McCarthy, M. C.; Cheng, L.; Crabtree, K. N.; Martinez, O.; Nguyen, T. L.; Womack, C. C.; Stanton, J. F. *J. Phys. Chem. Lett.* **2013**, *4*, 4133.
(8) Su, Y. T.; Huang, Y. H.; Witek, H. A.; Lee, Y. P. *Science* **2013**, *340*, 174.
(9) Li, J.; Carter, S.; Bowman, J. M.; Dawes, R.; Xie, D.; Guo, H. *J. Phys. Chem. Lett.* **2014**, *5*, 2364.
(10) Liu, F.; Beames, J. M.; Petit, A. S.; McCoy, A. B.; Lester, M. I. *Science* **2014**, *345*, 1596.
(11) Su, Y. T.; Lin, H.-Y.; Putikam, R.; Matsui, H.; Lin, M. C.; Lee, Y. P. *Nat. Chem.* **2014**, *6*, 477.
(12) Percival, C. J.; Welz, O.; Eskola, A. J.; Savee, J. D.; Osborn, D. L.; Topping, D. O.; Lowe, D.; Utembe, S. R.; Bacak, A.; M c Figgans, G.; Cooke, M. C.; Xiao, P.; Archibald, A. T.; Jenkin, M. E.; Derwent, R. G.; Riipinen, I.; Mok, D. W. K.; Lee, E. P. F.; Dyke, J. M.; Taatjes, C. A.; Shallcross, D. E. *Faraday Discuss.* **2013**, *165*, 45.
(13) Beames, J. M.; Liu, F.; Lu, L.; Lester, M. I. *J. Am. Chem. Soc.* **2012**, *134*, 20045.
(14) Beames, J. M.; Liu, F.; Lu, L.; Lester, M. I. *J. Chem. Phys.* **2013**, *138*, 244307.
(15) Lehman, J. H.; Li, H.; Beames, J. M.; Lester, M. I. *J. Chem. Phys.* **2013**, *139*, 141103.
(16) Sheps, L. *J. Phys. Chem. Lett.* **2013**, *4*, 4201.
(17) Ting, W.-L.; Chen, Y.-H.; Chao, W.; Smith, M. C.; Lin, J. J. *Phys. Chem. Chem. Phys.* **2014**, *16*, 10438.
(18) Smith, M. C.; Ting, W.-L.; Chang, C.-H.; Takahashi, K.; Boering, K. A.; Lin, J. J.-M. *J. Chem. Phys.* **2014**, *141*, 074302.
(19) Grebenshchikov, S. Y.; Qu, Z. W.; Zhu, H.; Schinke, R. *Phys. Chem. Chem. Phys.* **2007**, *9*, 2044.
(20) Aplincourt, P.; Henon, E.; Bohr, F.; Ruiz-Lopez, M. F. *Chem. Phys.* **2002**, *285*, 221.
(21) Lee, E. P. F.; Mok, D. K. W.; Shallcross, D. E.; Percival, C. J.; Osborn, D. L.; Taatjes, C. A.; Dyke, J. M. *Chem.—Eur. J.* **2012**, *18*, 12411.
(22) Meng, Q.; Meyer, H.-D. *J. Chem. Phys.* **2014**, *141*, 124309.
(23) Samanta, K.; Beames, J. M.; Lester, M. I.; Subotnik, J. E. *J. Chem. Phys.* **2014**, *141*, 134303.
(24) Deskevich, M. P.; Nesbitt, D. J.; Werner, H.-J. *J. Chem. Phys.* **2004**, *120*, 7281.
(25) Shiozaki, T.; Knizia, G.; Werner, H.-J. *J. Chem. Phys.* **2011**, *134*, 034113.
(26) Shiozaki, T.; Werner, H.-J. *Mol. Phys.* **2013**, *111*, 607.
(27) Kong, L.; Bischoff, F. A.; Valeev, E. F. *Chem. Rev.* **2011**, *112*, 75.
(28) Dawes, R.; Jasper, A. W.; Tao, C.; Richmond, C.; Mukarakate, C.; Kable, S. H.; Reid, S. A. *J. Phys. Chem. Lett.* **2010**, *1*, 641.
(29) Guo, H. *J. Chem. Phys.* **1998**, *108*, 2466.